

One-dimensional proton conductor under high vapor pressure condition employing titanate nanotube

Masanori Yamada¹, Mingdeng Wei, Itaru Honma, Haoshen Zhou^{*}

*Nano-energy Materials Group, Energy Technology Research Institute, National Institute of Advanced Industrial Science and Technology (AIST),
1-1-1 Umezono, Tsukuba, Ibaraki 305-8568, Japan*

Received 23 May 2006; received in revised form 12 July 2006; accepted 12 July 2006
Available online 14 August 2006

Abstract

Metal oxides with the nano-structure, such as nano-porous, -sheet, -particle, and -tube, have been attracted for the functional materials on the future technology. Especially, one-dimensional (1D) metal oxide nanotubes are emerging as potentially useful materials. In this paper, we prepared the 1D proton conductor under high vapor pressure condition employing titanate ($\text{H}_2\text{Ti}_3\text{O}_7$) nanotube (TNT). This metal oxide nanotube showed the proton conductivity of $5 \times 10^{-4} \text{ S cm}^{-1}$ at intermediate temperature ($\leq 160^\circ\text{C}$), fully saturated humidification (relative humidity of 100%), and high vapor pressure (6 atm) conditions. This conduction behavior in metal oxide nanotube is controlled by the liquid phase mediated charge transport (liquid-like mechanism). The proton conductor of 1D may have a potential not only for the fuel cell electrolytes operated at intermediate temperature conditions but also for various electrochemical devices. Furthermore, 1D proton conductor, such as TNT, might be used as the basic proton conductor to discuss the proton conductive mechanism.

© 2006 Elsevier B.V. All rights reserved.

Keywords: Proton conductivity; Nano-structure; Proton conductive electrolyte; Titanate; Metal oxide nanotube

1. Introduction

The proton conductor has been attracted for the electrolyte of proton exchange membrane fuel cell (PEFC). Especially, the operation of PEFC at intermediate temperature (100–200 °C) has been considered to provide many advantages, such as the reduction of amount of Pt electrode materials, improved CO tolerance, the higher energy efficiency, heat managements, and co-generations [1–4]. However, the hydrated perfluorosulfonic membranes, such as Nafion[®], are unstable at higher temperature (100 °C) and proton conductivity decreases by the evaporation of water from the membrane and degradations of the domain struc-

ture by irreversible reactions. Therefore, the development of a proton conductor with high proton conductivity at intermediate temperatures is necessary for solving problem in the current technologies [1–4].

Metal oxides with the nano-structure, such as nano-porous, -sheet, -particle, and -tube, have been attracted for the functional materials on the future technology [5,6]. Especially, metal oxide nanotubes are emerging as potentially useful materials. These nanotubes are unique one-dimensional (1D) nano-structures with uniform nanometer-sized channels possessing the high specific surface area. In addition, they are physically and chemically stable material and not dissolved in water [7,8]. Therefore, these metal oxide nanotubes are gradually attracting attention in the areas of solar cells, environmental protections, energy storages, gas sensors, catalyses, and biosensors [7–10]. However, the application of metal oxide nanotube for the electrolyte of PEFC has been hardly reported as far as we know.

^{*} Corresponding author. Tel.: +81 29 8615829; fax: +81 29 8615799.
E-mail address: hs.zhou@aist.go.jp (H. Zhou).

¹ Present address: Department of Chemistry, Faculty of Science, Okayama University of Science, Ridaicho, Okayama 700-0005, Japan.

Recently, the titanate ($\text{H}_2\text{Ti}_3\text{O}_7$) nanotube (TNT), which are composed of corrugated ribbons of edge-sharing TiO_6 octahedra, were synthesized [11,12]. The TNT can be prepared from polymorph of TiO_2 by a simple alkaline-hydrothermal treatment and subsequent acid washing. This TNT is different from the titania (TiO_2) nanotube and has a hydroxyl group on the TNT surface [10,13]. The hydrophilic TNT has a high water-holding capacity by the chemisorption and the surface of TNT can provide the aqueous-like environment. Therefore, the formation, structure, and stability of TNT for the proton conductor have been reported [14]. However, this research has been demonstrated under anhydrous condition and the specific property of TNT, such as high water-holding capacity by the chemisorption, was not used. Therefore, the proton conductivity of TNT at this condition was the order of $10^{-6} \text{ S cm}^{-1}$. Since the proton conductivity of the fully humidified TNT is controlled by the liquid phase mediated charge transfer (liquid like mechanism), the increase of conductivity is expected. Herein, we propose the utilization of TNT as a 1D proton conductor under saturated humidity condition (relative humidity of 100%; 100% RH). As a result, TNT indicate the proton conductivity of $5 \times 10^{-4} \text{ S cm}^{-1}$ at 160 °C under 100% RH condition. Additionally, these proton conductivities were stable at intermediate temperature, high humidity, and high vapor pressure conditions.

2. Experimental section

2.1. Preparation of titanate nanotubes (TNT)

TNT was synthesized based on a procedure with minor modification [11,12]. In a typical process, 1 g of TiO_2 powder (ST-01, obtained from Ishihara Sangyo Kaisha, Ltd.) and an aqueous solution of NaOH (10 M, 200 ml) were placed into a Teflon container. The mixture was vigorously stirred in an oil-bath at 100 °C for 72–120 h. The white suspension was filtrated and washed with dilute HCl and then deionized water until a pH value near 7 was obtained. Finally, the white product was dried at 60 °C for more than 3 h. Mesoporous silica was also synthesized by the reported procedure [15].

2.2. Characterization of titanate nanotubes

X-ray powder diffraction (XRD) patterns were recorded using a diffractometer MO3XHF22 (Mac Science Co., Ltd.). Multipoint Brunauer-Emmett-Teller (BET) surface area, pore volume, and Barret-Joyner-Halenda (BJH) pore size distribution of materials were calculated from the adsorption-desorption isotherm of N_2 at 77 K using a ASAP 2010 (Micromeritics Instrument Corp.). Both scanning electron microscope (SEM) and transmission electron microscope (TEM) measurements were conducted using a DS-720 (TOPCON Co. Ltd.) and a JEM-2000EXII (JEOL Co. Ltd.), respectively.

2.3. Conductivity measurements [16]

The powder samples were compacted into pellets. The pellet material was sandwiched between two gold electrodes. Proton conductivity was performed by the a.c. impedance method in a frequency range from 1 Hz to 1 MHz using an impedance analyzer SI-1260 (Solartron Co.) in a stainless steel vessel from RT to 160 °C. Conductivities of materials were determined from a typical impedance response (Cole–Cole plots). All the measurements in this experiment were carried out under fully saturated humidification condition (100% RH). Therefore, when the proton conductive measurements were demonstrated at higher temperature, the apparatus cell was pressurized to maximum 6 atm (160 °C) in order to keep saturated humidity [16].

3. Results and discussion

The TNT was synthesized by the previously reported procedures [11,12]. The BET surface area of TNT was $434 \text{ m}^2 \text{ g}^{-1}$. The SEM images of TNT have revealed the presence of numerous fiber-like products with typical lengths ranging from several hundreds nanometers to several tens micrometers, as shown in Fig. 1a. These fiber-like products lie close to each other, and their diameter is ca. 10 nm. In order to confirm the hollow nature of tubes, we demonstrated the TEM measurements of the same sample. Fig. 1b is a low magnification TEM showing a hollow nature of tubes. A high magnification image of a tube (Fig. 1b lower inset) revealed that the tube is a very crystallized multilayer wall with an inter-shell spacing of 0.7–0.8 nm, and the inner diameter is ca. <5 nm. It noticed that the tube is not symmetric. It has three layers for the upper side and four layers for the lower side. This indicates that the nanotube is achieved by scrolling process [11,12,17], and this is also evidenced by Fig. 1b upper inset, which shows a cross-sectional view of a single nanotube.

The powder sample of TNT were compacted into pellets and sandwiched between two gold electrodes. The proton conductivity measurements of the compacted pellets were demonstrated by the a.c. impedance method over the frequency range from 1 Hz to 1 MHz under fully saturated humidification condition (100% RH) [16]. In contrast, these samples did not indicate the electronic conductivity at the DC condition. Additionally, the diffusible ions other than proton have not existed in materials. Therefore, the measured impedance response indicates the proton conduction. Fig. 2a shows the typical impedance response (Cole–Cole plots) of TNT at 160 °C under 100% RH conditions. The Fig. 2b indicated the high frequency range (100 Hz–1 MHz) of TNT. Generally, the Cole–Cole plots corresponding to the lower conductivities show two well defined regions [18]: a semicircle passing through the origin in the high-frequency, which is related to conduction process in the bulk of the sample, and a

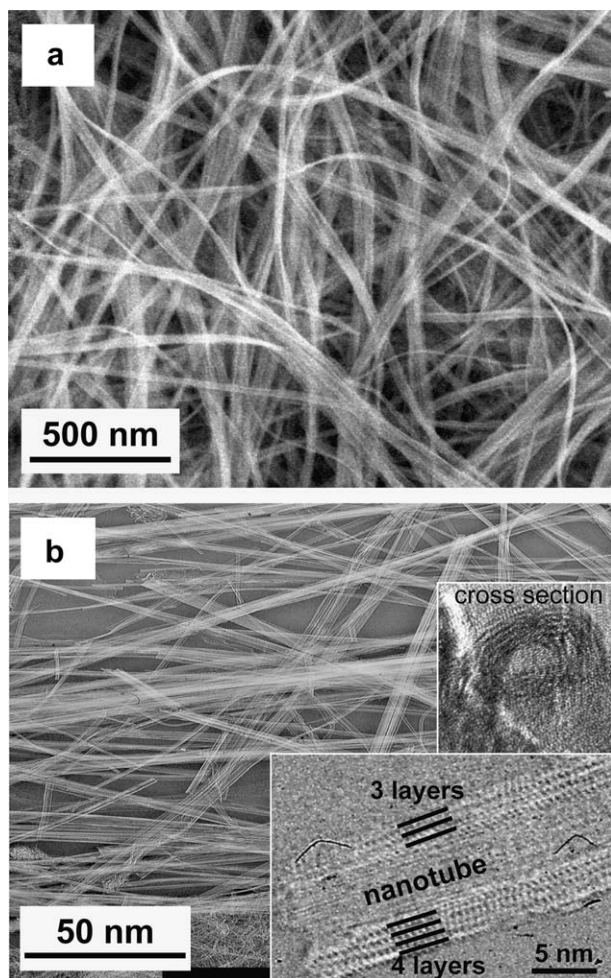


Fig. 1. (a) A SEM image of TNT. (b) A low magnification TEM image of TNT. The upper and lower inset indicated the cross section profile and high magnification images of TNT.

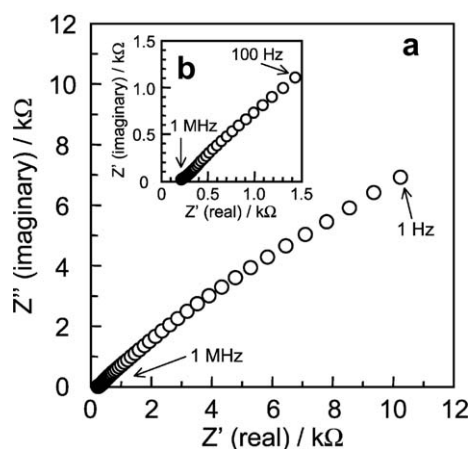


Fig. 2. Typical impedance response (Cole–Cole plots) of TNT at 160 °C under 100% RH conditions. Frequency range is from 1 Hz to 1 MHz. The insert indicated the high frequency range (100 Hz–1 MHz) of TNT.

monotonically decreasing curve with increasing frequency in the low-frequency that is attributed to the electrode/solid electrolyte interface. Therefore, the bulk resistance,

R_b , of material is obtained from the intercept of either curve (high frequencies semicircle or low frequencies tail) with the real axis [18]. However, in the material with high conductivities, a semicircle passing decrease with the increase of conductivity [19] and the bulk resistance, R_b , arise at the electrode/electrolyte interface [18]. In fact, a typical Cole–Cole plots of TNT showed a feature similar to that of the highly proton conducting membrane, such as Nafion® [20], the organic-inorganic hybrid membrane mixed with heteropolyacids [21], $\text{TiO}_2\text{--P}_2\text{O}_5$ material with the mesoporous structure [16], mesoporous TiO_2 [22], and biomolecule composite materials [23,24]. The resistances, R_b , of TNT were obtained from the extrapolation to the real axis.

Fig. 3 shows the proton conductivity of TNT in the temperatures range from RT to 160 °C under 100% RH conditions ((○) in Fig. 3). Additionally, we used also mesoporous silica, which can hold physisorbed water, as a comparative material ((△) in Fig. 3) [16]. The proton conductivities of TNT lightly increased with the increase of cell temperature and reached a maximum conductivity at 160 °C. The maximum proton conductivity was $5 \times 10^{-4} \text{ S cm}^{-1}$. This proton conductivity under fully humidified condition was two order higher than that of TNT under anhydrous condition [14]. Additionally, this proton conduction was stable and maintained for several hours at same conditions. This result suggested the TNT was proton conductive material and stable at the intermediate temperature (≤ 160 °C), high humidity, and high vapor pressure conditions. In contrast, the conductivity of mesoporous silica, which can hold physisorbed water, slightly decreased with the increase of temperature because the hydrate water in pore structure evaporates [16]. Additionally, at high temperature condition (above 100 °C), the proton conductivity of Nafion® decreases by the evaporation of water from the membrane and degradations of the domain structure by irreversible reactions. Therefore, the water holding by the chemisorption and the thermal stability at high temperature condition is important for the proton transfer. Next, to discuss the proton transfer mechanism in TNT, we determined the activation energy (E_a) of proton conduction. Fig. 4 shows the Arrhenius

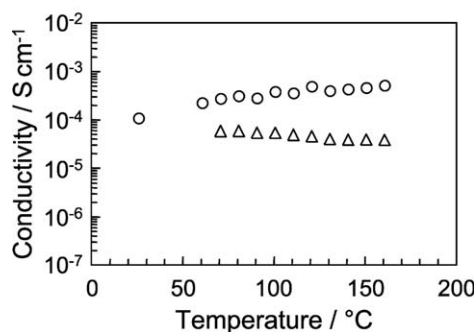


Fig. 3. Proton conductivity of (○) TNT and (△) mesoporous silica from RT to 160 °C under 100% RH condition.

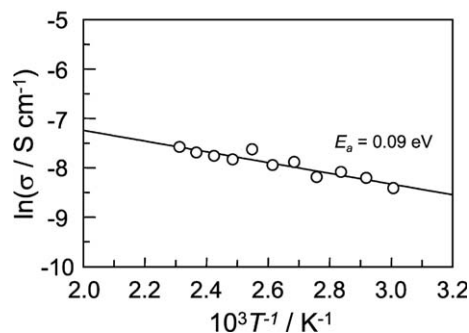


Fig. 4. Arrhenius plots of the conductivity of TNT. Solid lines are results of the least-squares fitting. Activation energies (E_a) of the proton transport under 100% RH condition were estimated from the slope.

plot of proton conductivity of TNT. Solid lines in Fig. 4 are the results of the least-squares fitting. The E_a of proton conduction were estimated from the slope. The E_a of proton conduction of TNT was 0.09 eV. In contrast, mesoporous silica could not calculate the E_a since the proton conductivity decreased with the increase of temperature. The E_a value of TNT is almost same as that of humidified Nafion[®] [20] and TiO₂–P₂O₅ self-ordered, crystalline-glass, mesoporous nanocomposite (CGMN) [16]. This E_a is lower than that of anhydrous proton conductor (E_a ; >0.2 eV) based on proton hopping mechanism [22–25]. In fact, the proton conductivity and E_a of TNT under anhydrous condition has been reported the order of 10^{-6} S cm⁻¹ and 0.57 eV, respectively [14]. These results suggest that the conduction behavior is controlled by the liquid phase mediated charge transport (liquid-like mechanism), such as H₃O⁺ or H₃O₂⁺ [25,26].

It is known that the inorganic proton conductors, such as metal oxide hydrate [25,27] or solid acids [28], show the high proton conduction. However, at the intermediate temperature condition, the proton conductivity of metal oxide hydrate decreases since the hydrate water evaporates from the material [25,27]. Additionally, at the high humidity and high vapor pressure conditions, the solid acid and metal oxide hydrate with the high water solubility are not so stable and dissolved in water. Therefore, the high water holding capacity, thermal stability, and low solubility in water is important factor for the electrolyte of PEFC. On the other hand, metal oxide nanotubes are water-insoluble and thermo-stable materials. In fact, these nanotubes have been synthesized by the hydrothermal treatment [11,12]. Furthermore, titanate (H₂Ti₃O₇) nanotube (TNT) is different from the titania (TiO₂) nanotube and has a hydroxyl group on the TNT surface [10,13]. Therefore, the surface of TNT has a high water-holding capacity and one TNT material acts as 1D proton conductor with the liquid phase. As a result, TNT indicated the proton conductivity of 5×10^{-4} S cm⁻¹ with the thermal stability at intermediate temperature under 100% RH conditions.

4. Conclusion

In summary, we prepared the 1D proton conductor of 1D employing titanate (H₂Ti₃O₇) nanotube (TNT). This TNT showed the proton conductivity of order of 10^{-4} S cm⁻¹ at intermediate temperature (≤ 160 °C), fully saturated humidification (100% RH), and high vapor pressure (6 atm) conditions. The proton conductor of one-dimension may have a potential not only for the fuel cell electrolytes operated at intermediate temperature conditions but also for the electrochemical devices including chemical sensors, lithium rechargeable battery, and others. Furthermore, one dimensional proton conductor, such as TNT, might be used as the basic proton conductor to discuss the proton conductive mechanism.

References

- [1] Q. Li, R. He, J.O. Jensen, N.J. Bjerrum, *Chem. Mater.* 15 (2003) 4896.
- [2] M.A. Hickner, H. Ghassemi, Y.S. Kim, B.R. Einsla, J.E. McGrath, *Chem. Rev.* 104 (2004) 4587.
- [3] W.H.J. Hogarth, J.C.D. Costa, G.O. Lu, *J. Power Sources* 142 (2005) 223.
- [4] M.A. Hickner, H. Ghassemi, Y.S. Kim, B.R. Einsla, J.E. McGrath, *Chem. Rev.* 104 (2004) 4587.
- [5] U. Bach, D. Lupo, P. Comte, J.E. Moser, F. Welssörtels, J. Scallbeck, H. Spreitzer, M. Grätzel, *Nature* 395 (1998) 583.
- [6] M. Wagemaker, A.P. Kentgens, F.M. Mulder, *Nature* 418 (2002) 397.
- [7] G.R. Patzke, F. Krumeich, R. Nesper, *Angew. Chem. Int. Ed.* 41 (2002) 2446.
- [8] R. Ma, Y. Bando, T. Sasaki, *J. Phys. Chem. B* 108 (2004) 2115.
- [9] M. Wei, Y. Konishi, H.S. Zhou, H. Sugihara, H. Arakawa, *J. Electrochem. Soc.* 153 (2006) A1232.
- [10] A. Liu, M. Wei, I. Honma, H.S. Zhou, *Anal. Chem.* 77 (2005) 8068.
- [11] T. Kasuga, M. Hiramatsu, A. Hoson, T. Sekino, K. Niihara, *Langmuir* 14 (1998) 3160.
- [12] B.D. Yao, Y.F. Chan, X.Y. Zhang, W.F. Zhang, Z.Y. Yang, N. Wang, *Appl. Phys. Lett.* 82 (2003) 281.
- [13] A. Corma, V. Fornes, F. Rey, *Adv. Mater.* 14 (2002) 71.
- [14] A. Thorne, A. Kruth, D. Tunstall, J.T.S. Irvine, W. Zhou, *J. Phys. Chem. B* 109 (2005) 5439.
- [15] D. Zhao, J. Feng, Q. Huo, N. Melosh, G.H. Fredrickson, B.F. Chmelka, G.D. Stucky, *Science* 279 (1998) 548.
- [16] M. Yamada, D. Li, I. Honma, H.S. Zhou, *J. Am. Chem. Soc.* 127 (2005) 13092.
- [17] Y.Q. Wang, G.Q. Hu, X.F. Duan, H.L. Sun, Q.K. Xue, *Chem. Phys. Lett.* 365 (2002) 427.
- [18] M.A. Vargas, R.A. Vargas, B.-E. Mellander, *Electrochim. Acta* 44 (1999) 4227.
- [19] M. Yamada, I. Honma, *J. Phys. Chem. B* 108 (2004) 5522.
- [20] Y. Sone, P. Ekdunge, D. Simonsson, *J. Electrochem. Soc.* 143 (1996) 1254.
- [21] I. Honma, H. Nakajima, O. Nishikawa, T. Sugimoto, S. Nomura, *Solid State Ionics* 162–163 (2003) 237.
- [22] F.M. Vichi, M.I. Tejedor-Tejedor, M.A. Anderson, *Chem. Mater.* 12 (2000) 1762.
- [23] M. Yamada, I. Honma, *Angew. Chem. Int. Ed.* 43 (2004) 3688.
- [24] M. Yamada, I. Honma, *ChemPhysChem* 5 (2004) 724.
- [25] P. Colomban, A. Novak, *J. Mol. Struct.* 177 (1988) 277.
- [26] K.D. Kreuer, *Chem. Mater.* 8 (1996) 610.
- [27] O. Nakamura, T. Kodama, I. Ogino, Y. Miyake, *Chem. Lett.* (1979) 17.
- [28] S.M. Haile, D.A. Boysen, C.R.I. Chisholm, R.B. Merle, *Nature* 410 (2001) 910.